BioMetals 1995, **8**, 246–256

Cellular and subcellular localization of chromium in the crab *Liocarcinus puber* (Brachyrhyncha) by transmission electron microscopy, secondary ion mass spectrometry and electron microprobe analysis

Colette Chassard-Bouchaud*,†, Michelle Hubert*, Françoise Escaig† & René Louis Inglebert‡

**Laboratoire de Biologie et Physiologie des Organismes marins, Université Pierre et Marie Curie, Paris, France, †Centre de Microanalyse appliquée à la Biologie (INSERM SC 27) du Laboratoire de Biophysique de la Faculté de Médecine, Créteil, France and ‡Groupe de Recherches sur l'Energétique des Milieux Ionisés, CNRS, URA 831, Université d'Orléans, Orléans, France*

Received 14 July 1994; accepted for publication 15 December 1994

The swimming crab *Liocarcinus puber* (Crustacea Brachyrhyncha) was exposed for 2 weeks to $CrCl_3$ (chromium occurs principally in the trivalent state in the natural environment). The gills, digestive gland and muscle were examined by several analytical techniques for cellular and subcellular localization of chromium. The techniques applied were secondary ion mass spectrometry (ion microscopy and ion microprobe analysis) associated with photon microscopy and X-ray spectrometry (electron microprobe analysis) together with transmission electron microscopy. The digestive gland was found to be free of chromium, whereas chromium was adsorbed onto the gill exoskeleton. The muscle was the only tissue with intracellular electron-dense precipitates with no surrounding membrane. The metal was detected in the heterophagic vacuoles of amoebocytes where it was associated with phosphorus and trapped in an unsoluble form. Mechanisms of chromium cellular and subcellular metabolism were compared between crabs and other aquatic organisms. *L. puber* does not appear to be a suitable bioindicator of chromium pollution because of molting and its low chromium bioaccumulation capability.

Keywords: bioaccumulation, chromium, crab, mass spectrometry, X-ray microanalysis

Introduction

Coastal waters adjacent to large population centers receive a variety of wastes as a result of many anthropogenic inputs, e.g. domestic wastewaters, manufacturing processes, atmospheric fallouts and sewage sludge productions. Many of these components are harmful to marine biota, among which are organisms of interest such as bivalve molluscs, decapod crustaceans and teleost fish that act as bioindicators of water quality and are also edible species. It is well known that these organisms can concentrate toxicants through uptake from water and sediments (as dissolved or particulate matter) which enter the organisms via the gills, digestive tract or integument. Contaminants are then stored in various tissues and organs (among which, one or several targets are generally determined) which will be used then as indicator organs (Chassard-Bouchaud 1993).

Among the trace metal contaminants, the element chromium is very toxic. The ability of marine organisms to accumulate chromium from ambient seawater is well documented (Fukai & Broquet 1965). Chromium is an element found in many minerals distributed in the Earth's crust, and it may enter rivers and the sea through run-off after rain and land subsidence. It has to be noticed that chromium is also essential for life, together with 10 other trace elements (Kieffer 1979), e.g. for the biosynthesis of the glucose tolerant factor.

During recent decades, increased quantities of chromium compounds have been used by man. The anthropogenic input of chromium into the aquatic ecosystem is about 142 000 tons $year^{-1}$ [in third position after manganese (262 000 tons) and zinc (226 000 tons); Nriagu & Pacina 1988].

Chromium (atomic number 24 and atomic mass 51.996)

Address for correspondence: Colette Chassard-Bouchaud, Laboratoire de Biologie et Physiologie des Organismes Marins, boîte Courrier 006, Université Pierre et Marie Curie, 4, place Jussieu, F-75252, Paris Cedex 05, France. Fax: (+33) 1 44 27 52 50.

exists in all oxidation states from II to VI, but only the trivalent and hexavalent compounds and the metallic chromium are of practical importance. The naturally occurring isotopic mixture consists of four isotopes with ^{52}Cr as the main isotope (83.76%) as well as ^{50}Cr (4.31%), ^{53}Cr (9.55%) and ^{54}Cr (2.38%). The danger of chromium environmental contamination depends on its oxidation state. In its hexavalent form it is 100 to 1000 times more toxic than most trivalent compounds.

In a previous paper, we were able to present extensive results on chromium bioaccumulation in the marine mussel *Mytilus edulis* (Chassard-Bouchaud *et al.* 1989). Data were obtained on the uptake, distribution and loss of chromium at the light microscopic and electron microscopic levels, using associated microanalytical techniques. Chromium detection was as follows: kidney and gills exhibited the highest values, intermediate values were found for muscle and byssus (chromium was adsorbed onto the threads and was incorporated within them), and lowest values were found in the digestive gland. Chromium was also detected in amoebocytes where the target organelles of metal accumulation were the lysosomes. In these organelles, chromium was associated with phosphorus and trapped in an insoluble form.

Consequently, it appeared to us of interest to compare results obtained from chromium bioaccumulation in bivalves with results obtained from other bioindicators such as Crustaceans. These animals belong to an unusually diverse and widespread group which encompasses marine species of major economic importance such as crabs, shrimps and prawns, which are often intermediary links in the food web. Literature provides quantitative data of chromium concentration in several species of decapods with the following values: *Portunus holsatus*, whole animal, 0.33 mg kg^{-1} fresh weight (De Clerck *et al.* 1979); *Cancer irroratus*, gill: 0.8–2.5, digestive gland: 0.5–1.2, flesh: 0.3–0.6 (Greig *et al.* 1977); *Jasus lalandi*, flesh: 0.08–0.11 (Van As *et al.* 1975); *Paralithodes kamtschatica*, flesh: 0.09 (Fukai & Broquet 1965); carapace of *Eriphia verrucosa*, 0.4; and carapace of *Parapeneus longirostris*, 0.5 (Bernhard & Zattera 1975). From these data, it appears that chromium levels are rather low. Moreover, several tissues and organs exhibit a bioaccumulation ability which may be either a real intracellular concentration or only a surface adsorption, as suggested by Tennant & Forster (1969) working on chromium concentration in the crab *Cancer magister*.

The biochemical methods commonly used are inadequate to answer these questions, as absorbed and unabsorbed elements cannot be distinguished. In addition, long-term investigations or other analytical methods are needed. The available microanalytical techniques are more suitable. Secondary ion mass spectrometry (SIMS), usually called SIMS microscopy, and X-ray spectrometry enable both simultaneous morphological and chemical identification in histological sections.

X-ray microanalysis, also called electron microprobe analysis (EMPA), is associated with transmission electron microscopy. This system provides a means for studying the local composition and structure of cells and organelles at the micro-size scale. Although EMPA is the most often used method, many biological problems cannot be studied because of its relatively low sensitivity and its inability to detect light elements.

In SIMS, a primary ion beam is focused on the specimen surface, resulting in the production of positive and negative ions from the surface layer of the section. The secondary ions are extracted from the specimen and analyzed in a mass spectrometer. The analytical ion microscope was invented by Castaing & Slodzian (1962) based on SIMS. Using the analytical ion microscope, the observer can visualize and focus on an area in a histological section of tissue, analyze its chemical contents and photograph the microscopical distribution of any element in that area of tissue. The analytical ion microscope consists of two components: (1) an ion microscope with which the observer chooses an area of interest in the histological section and (2) a mass spectrometer, which identifies the atoms present in the selected area.

There are two types of SIMS instrument. The first type is the analytical ion microscope, which has a large beam to bombard an area 30–400 μm in diameter. There is no scanning to form the image of the distribution of the secondary ions, which is obtained with appropriate ion optics. The second type of instrument is the ion microprobe, which scans the surface of the tissue with an ion beam measuring less than 2 μm in diameter to form an image of the tissue examined. The distribution of an ion is visualized by calibrating the instrument to accept only pulses of the particular ion chosen. The atoms thus excited become secondary ions which are analyzed by the mass spectrometer as above.

The main advantage of SIMS as applied in biological research is its very high sensitivity—more than 1000 to 10 000 times higher than that of the EMPA (Chassard-Bouchaud 1991). Moreover, images representing the distribution of all of the elements of the periodic table are easily obtained, even when concentrations are very low (0.1 $\mu g\, g^{-1}$).

We were able to demonstrate by our previous data that these microanalytical techniques are particularly useful for investigations in marine toxicology (Chassard-Bouchaud 1991). The present report has three purposes. (1) to obtain precise information on the localization of chromium at the structural and ultrastructural levels in a decapod crustacea, using microanalytical techniques. The crab *Liocarcinus puber* was chosen because it is a common and edible species from the French Mediterranean coast. (2) To compare the results of the present study with the findings obtained previously from the mussel *M. edulis*, using the same analytical techniques. (3) To determine if *L. puber* was a suitable indicator species for chromium contamination.

Materials and methods

Biological material

Mature specimens of *L. puber* with a carapace 60 mm in width were collected from coastal waters of the Mediterranean (Villefranche-sur-Mer, France). Two groups of five male

crabs and two groups of five female crabs were chosen at the C stage of the intermolt cycle (C stage being the period of steadiness: Drach & Tchernigovtzeff 1967). They were kept in an aquaria with 40 l of aerated sea water (36% salinity at 12°C). Crabs were exposed to $CrCl_3$ at a concentration of 10 mg l^{-1} for 2 weeks as chromium occurs principally in the trivalent state in the natural environment. During the experiments, both the water and the metal were changed daily. The crabs were then dissected to separate the different tissues, which then underwent several treatments depending on the microanalytical technique to be used.

For SIMS, tissues were fixed chemically in Carnoy's fixative, embedded in paraffin, cut to sections (5 μm) and deposited on a high purity gold specimen holder, with removal of paraffin. Alternatively, cryofixation was performed with isopropane and then liquid nitrogen, and sections were deposited on gold specimen holders.

For X-ray analysis, samples were fixed in 2.5% glutaraldehyde in 0.2 M sodium dimethylarsinate buffer at pH 7.0. After washing with the buffer, the samples were dehydrated and embedded in Epon. Ultrathin sections were then deposited on copper grids and coated with carbon. Grids to be observed by electron microscopy were stained (uranyl acetate and lead citrate) while grids to be examined with the electron microprobe were unstained.

Cryofixation and both chemical fixations were performed on each tissue of the 20 samples. The gills, the digestive gland and the muscle of control and chromium-exposed *L. puber* were analyzed by photon and by transmission electron microscopy. Simultaneously, metal analyses of each tissue were performed at the structural level, using SIMS (ion microscopy and ion microprobe analysis), and at the ultrastructural level, using X-ray analysis (EMPA).

Instrumentation

Electron microscopy. A Philips EM 300 transmission electron microscope was used to study the ultrastructure of tissue sections.

SIMS. SIMS was performed using an ion microscope and an ion microprobe.

The *ion microscope* (Cameca IMS 300) was equipped with an electrostatic deflector with O_2^+ as primary ions. The images of the distribution of the secondary ions were obtained directly with appropriate ion optics. Ion microscopy imaging, giving the chromium distribution in the tissue sections, was performed using a beam of uniform density bombarding a large area (250 μm). The analytical conditions were previously described (Chassard-Bouchaud *et al.* 1992). SIMS high mass resolution spectra were recorded in order to make the distinction between monoatomic ions and polyatomic ions at a given mass. At mass 52, it is necessary to make the distinction between the $^{52}Cr^+$ ion and polyatomic ions (principally CaC: 40 + 12).

A Riber MIQ 256 *ion microprobe* (Outrequin *et al.* 1988) with its associated equipment, including a pollution-free ultrahigh vacuum system, was used with a liquid metal gallium ion source (primary ions) for the study of positive secondary ions. Secondary ions were examined with a high-sensitivity quadrupole mass spectrometer. The surface of the specimen was scanned by a focused primary ion beam to obtain images.

X-ray spectrometry. A Camebax microprobe, associated with a transmission electron microscope, was used to identify elements within ultrathin sections. It was equipped with a two wavelength-dispersive spectrometer fitted with the following crystals: TAP, ODPB, PET and LIF. The analytical conditions were previously described (Chassard-Bouchaud *et al.* 1992).

In addition, the relative metal concentration at the subcellular level, was estimated by determining the number of counts from the K_α line of chromium and phosphorus over 50 s. Counts on 20 organelles of 10 individuals were used to obtain the mean of each measurement. The background was determined by shifting the spectrometer to both sides of the line.

Results

Gills

Photon micrographs (Figures 1a and 2a) show cross-sections of gills of a chromium-exposed crab with the axis bearing several lamellae covered by the cuticle. Two sets of SIMS images were obtained from those lamellae. The first set corresponds to the calcium distribution (Figures 1b and 2b), which represents the general topography of the section as calcium is the major mineral component, regularly distributed, of the crustacean tissues. The second set, obtained from the same area of the section, presents the chromium distribution (Figures 1c and 2c). In Figure 1(c), the brightness of the amoebocyte is significant of its high chromium content. A low resolution mass spectrum (Figure 3) was obtained from this specialized type of cell: all stable isotopes of chromium were identified [$^{50}Cr^+$ (4.31%), $^{52}Cr^+$ (83.76%, major isotope), $^{53}Cr^+$ (9.55%) and $^{54}Cr^+$ (2.38%)].

The surface of the cuticle exhibits a high chromium emission (Figure 2c). However, these data, obtained at the structural level, required further investigation in order to determine the precise localization of chromium. Consequently, the same samples were investigated using transmission electron microscopy. Figure 4 presents the ultrastructural aspect of a gill lamella with epithelial cells and the cuticle they have secreted, covered by the epicuticle overlapped by an irregular layer of electron dense precipitates with a mean diameter of 37 nm. Using the electron microprobe, we were able to demonstrate that these deposits were composed of chromium associated with phosphorus (Figure 4, inset).

Measurements of the element concentration (Figure 5) performed on the gills are given by the number of counts (over 50 s): chromium associated with phosphorous is exclusively present at the surface of the epicuticle in those dense deposits, while the cuticle itself and the lysosomes are free of chromium.

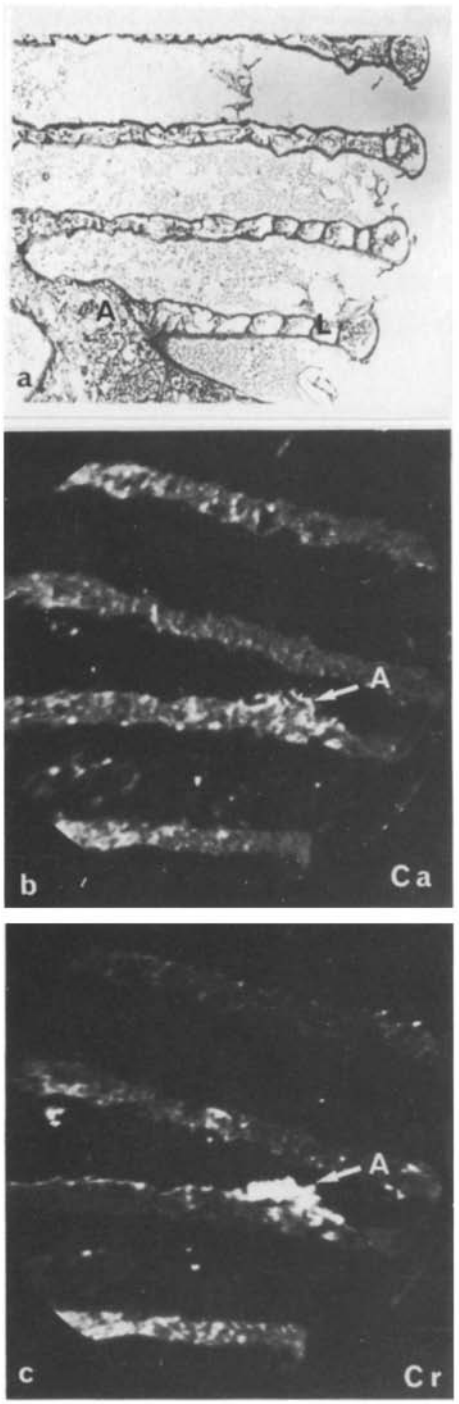

Figure 1. *L. puber.* Chromium-exposed gill. (**a**) Photon micrograph of semithin cross-section showing the axis (A) of the gill with numerous lamellae (L); × 560. (**b**) $^{40}Ca^{+}$ SIMS image showing topography of the section with gill lamellae and an amoebocyte (A); × 560. (**c**) $^{52}Cr^{+}$ SIMS image obtained from the same area as (**b**) showing the high chromium emission from the amoebocyte (A) which appears very bright; × 560.

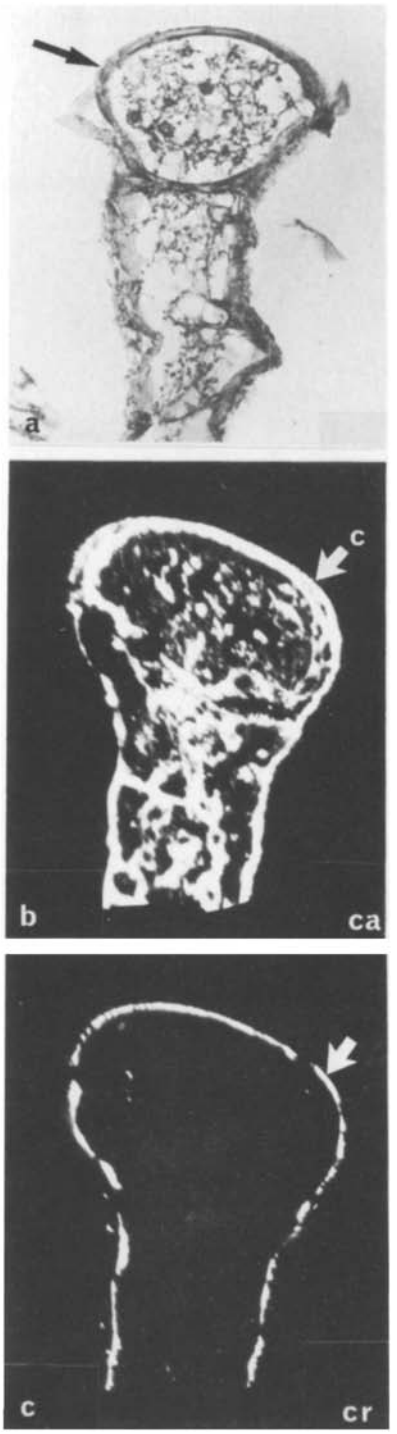

Figure 2. *L. puber.* Chromium-exposed gill. (**a**) Photon micrograph of the apical area of the lamella with epidermis covered by the cuticle (arrow); × 2310. (**b**) $^{40}Ca^{+}$ SIMS image showing topography of the section with epidermis covered by cuticle (c); × 2310. (**c**) $^{52}Cr^{+}$ SIMS image obtained from the same area as (**b**) showing the higher chromium emission from the surface of the cuticle (arrow); × 2310.

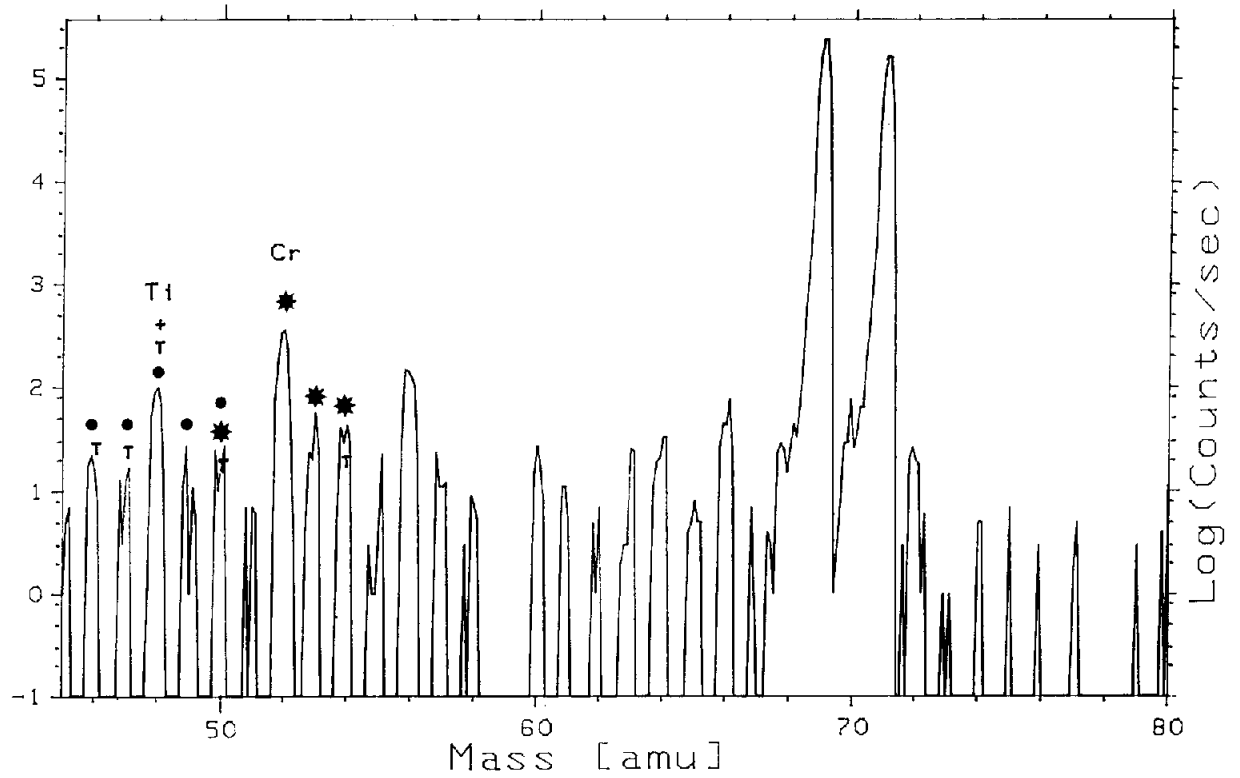

Figure 3. *L. puber*. Chromium-exposed gill. Ion microprobe spectrum showing the four stable isotopes of chromium (★) of masses 50 (4.31%), 52 (major isotope 83.76%), 53 (9.55%) and 54 (2.38%). Note the presence of titanium isotopes (●) and gallium isotopes 69 (60.40%) and 71 (39.60%) due to the liquid gallium primary ion source.

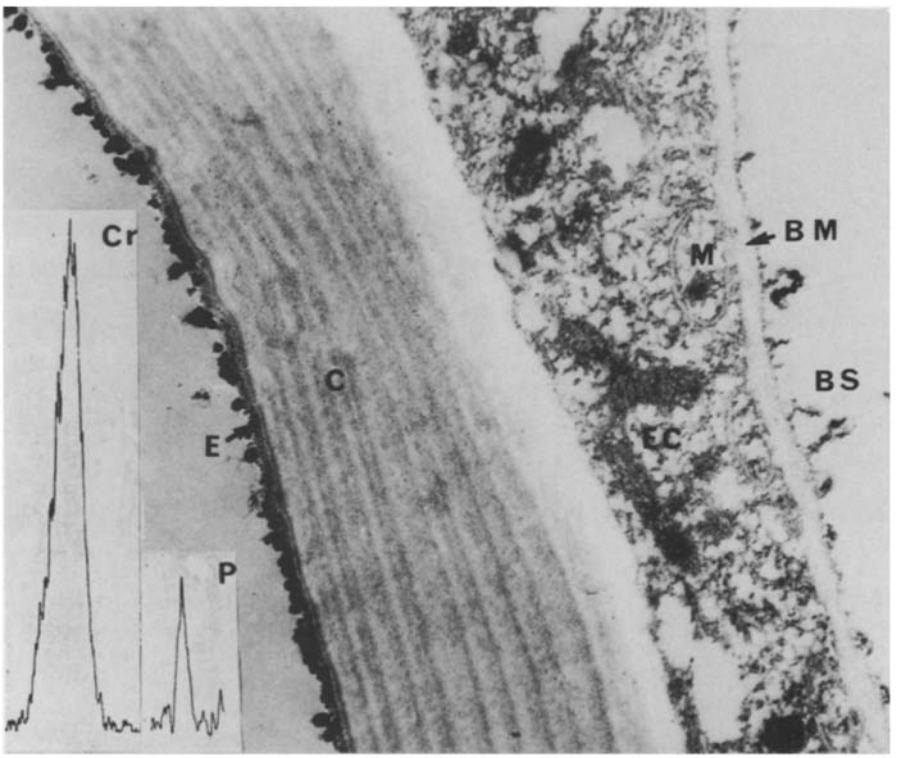

Figure 4. *L. puber*. Chromium-exposed gill. Electron micrograph of a lamella showing epithelial cells (EC) with mitochondria (M), basement membrane (BM) and cuticle (C) covered by the epicuticle (E) lining outer surface and showing chromium dense deposits (arrows). BS, blood space. × 37 800. Inset: X-ray emission spectra of chromium and phosphorus (K_α line) obtained from these dense deposits covering the epicuticle.

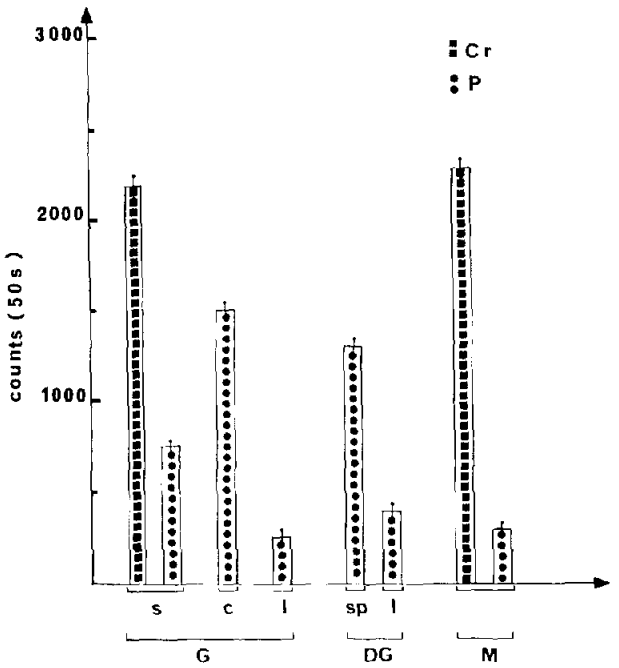

Figure 5. *L. puber*. Chromium-exposed crabs. Tissue distribution of chromium and phosphorus obtained by X-ray microanalysis (EMPA). Elements were detected from the following. Gill (G): chromium associated with phosphorus was present at the surface (s) of the epicuticle while cuticle (c) and lysosomes (l) were free of chromium. Digestive gland (DG): spherocrystals (sp) and lysosomes (l) were free of chromium. Muscle (M): non-membrane limited microprecipitates were shown to contain chromium associated with phosphorus. Bars represent means and standard deviation from measurements on 20 organelles from 10 individuals.

Moreover, it appears that the gill ultrastructure does not seem to be altered by chromium exposure.

Digestive gland

The photon micrographs obtained from cross-sections of digestive gland diverticula show a normal structure. Observations performed at the ultrastructural level confirm this unaffected aspect of the epithelial cells with numerous mitochondria and microvilli, while the basal area was crowded with spherocrystals (Figure 6).

Spherocrystals, also known as 'calcium phosphate granules', are well known mineral concretions, commonly distributed in many invertebrates such as arthropods and molluscs. X-ray microanalysis performed at this ultrastructural level gave negative results: spherocrystals together with lysosomes were completely free of chromium (Figure 5). These data were confirmed by the high mass resolution spectrum obtained at mass 52 ' from this digestive gland, showing a high CaC peak and only a faint peak of chromium corresponding to constitutive chromium which is always present (Figure 10).

Muscle

Samples of walking leg muscle were examined and analyzed at the ultrastructural level: it appears that chromium contamination did not induce cellular alteration. Figure 8 indicates the presence of electron-dense precipitates with a mean diameter of 60 nm with no surrounding membrane: they lie in between the myofibrils. These precipitates were

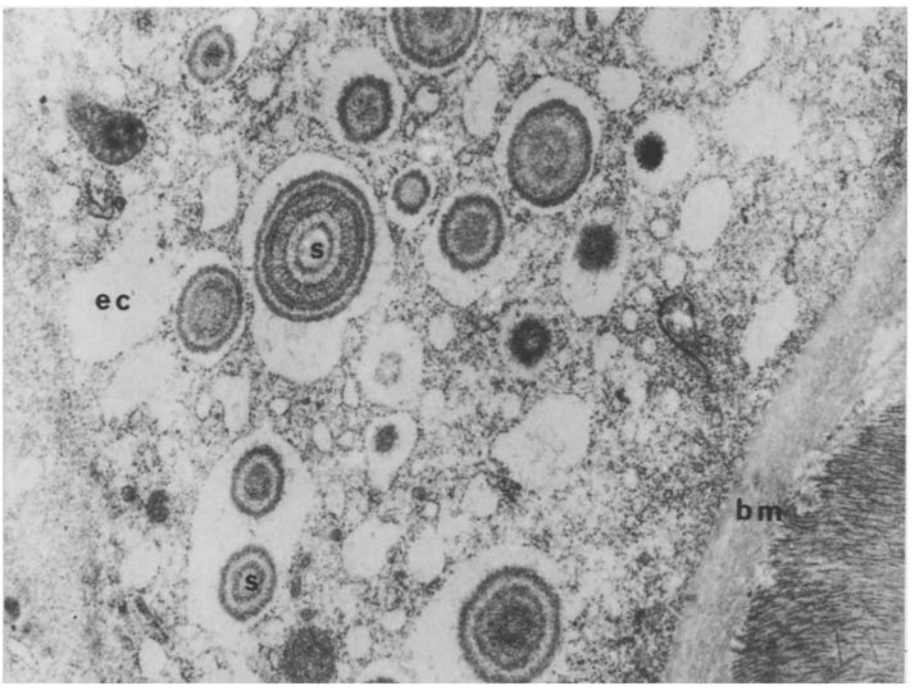

Figure 6. *L. puber*. Chromium-exposed digestive gland. Electron micrograph of basal area of epithelial cells (ec) showing spherocrystals (s) and basement membrane (bm); ×22400.

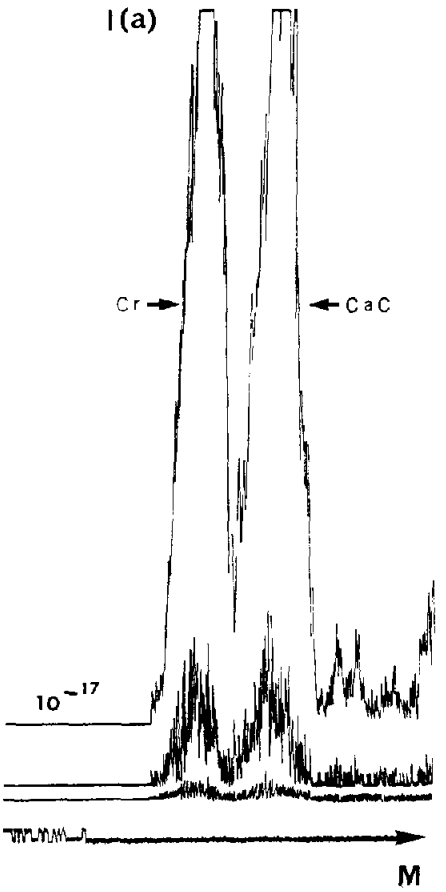

Figure 7. *L. puber.* Chromium-exposed amoebocytes. Ion microscope spectrum. High mass resolution at 52^+ showing abundance of chromium and the contribution of polyatomic ions CaC. I, intensity (A); M, mass.

analyzed using the electron microprobe: typical chromium and phosphorus peaks were obtained (Figure 8, inset). Measurements demonstrate that the highest chromium levels, in all recorded spectra, were obtained from these microgranules (Figure 5).

Amoebocytes

Amoebocytes are large phagocytic cells which play an important role in detoxifying processes. Using their numerous pseudopods, they migrate through the different tissues and engulf, by endocytosis, foreign particles. They are distributed throughout the hemolymph system. As the vascular system is semiclosed, these cells are also found within the organs as well as at their outer surface, as seen in Figures 1(b and c) on gill lamellae. Moving by diapedesis, they can cross epithelial layers. Figure 9 presents several amoebocytes exhibiting heterophagic vacuoles containing large electron-dense deposits. Using ion microscopy, it was possible to demonstrate that these deposits consisted of chromium associated with phosphorous; the high mass resolution spectrum obtained at mass 52^+ (Figure 7) from this section exhibits a high peak of chromium associated with a peak corresponding to the contribution of polyatomic CaC ions.

Discussion

Our investigations were performed using two types of fixation techniques: classical chemical techniques and cryofixation. Both the chemically fixed and the frozen sections were investigated using a photon and an electron microscope and the microanalytical systems. As the quality of the images obtained from the frozen sections was mediocre because of artifacts due to the surface of frozen sections not being perfectly flat and equipotential, this did not allow us to obtain the best results. As the analytical and ultrastructural results obtained using cryofixation techniques were comparable to those obtained using chemical techniques, we present micrographs obtained by the latter type of fixation which are of better quality.

Concerning both SIMS techniques, the ion microscope presents the advantage of ion images of a better resolution than those obtained from the ion microprobe; conversely, ion microprobe analysis is more sensitive (Chassard-Bouchaud 1991).

The subcellular distribution of elements can be investigated by cell fractionation, a procedure which is based on differential pelleting homogenates. On the other hand, it does not give true purified subcellular particles as such, but fractions enriched in particular organelles such as nuclei, mitochondria or lysosomes.

Two facts have to be considered. (1) The enrichment is dependent on the method used and varies from one tissue to another, and thus would be inadequate and not precise enough for our purpose. (2) According to our results obtained from non-membrame limited chromium microprecipitates located within the crab muscle, it appears that the fractionation technique would not have been suitable. No procedures other than the microanalytical techniques presented and used in this present report would provide a suitable method for studying the local elemental composition of biological specimens, on the micron- and submicron-size scale.

The toxicity of chromium is generally well documented in the literature with reference to vertebrates (Langård 1982, Allan 1988) and, particularly, to fish (see references in Chassard-Bouchaud *et al.* 1989). As chromium salts are active at low concentrations and are toxic to fish, e.g. at a 0.1 p.p.m. dose (Strik *et al.* 1975), investigations on this metal require very sensitivie instruments.

Little information is available on chromium toxicity to invertebrates. Concerning molluscs, available data were quoted in our previous paper (Chassard-Bouchaud *et al.* 1989) devoted to chromium uptake, distribution and loss in the mussel *M. edulis*, which is well known as a good indicative species of marine pollution. Using the same microanalytical techniques as those described above, investigations were

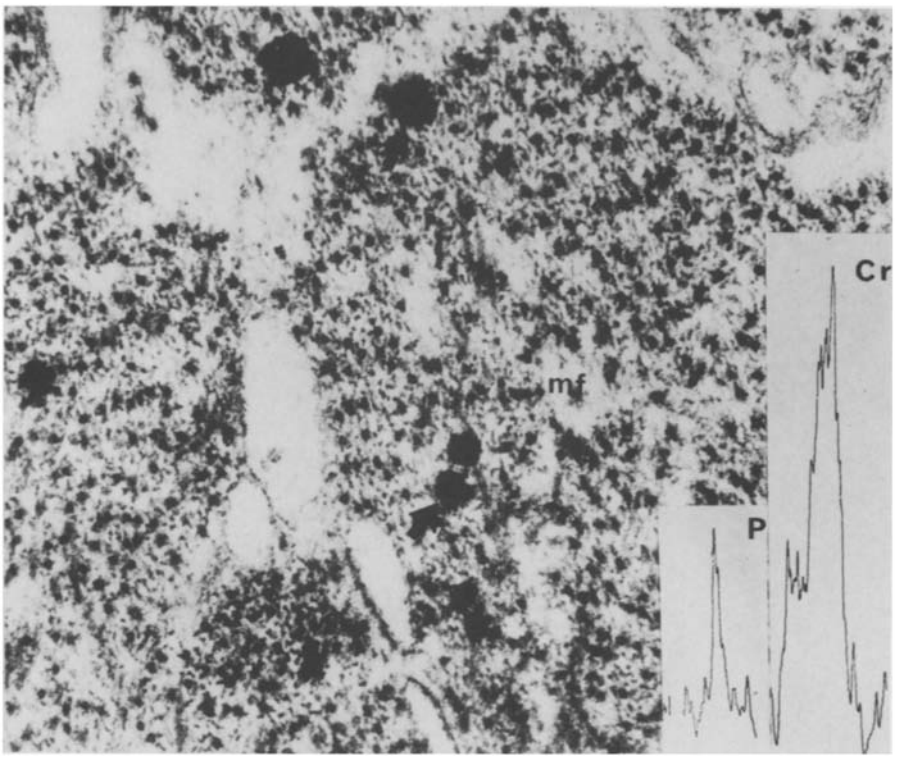

Figure 8. *L. puber*. Chromium-exposed muscle. Electron micrograph of cross-section of walking leg muscle fiber which is made up of myofibrils (mf) where chromium and phosphorus microprecipitates (arrows) were detected: ×58 800. Inset: X-ray emission spectra of chromium and phosphorus (K_γ line) obtained from these microprecipitates.

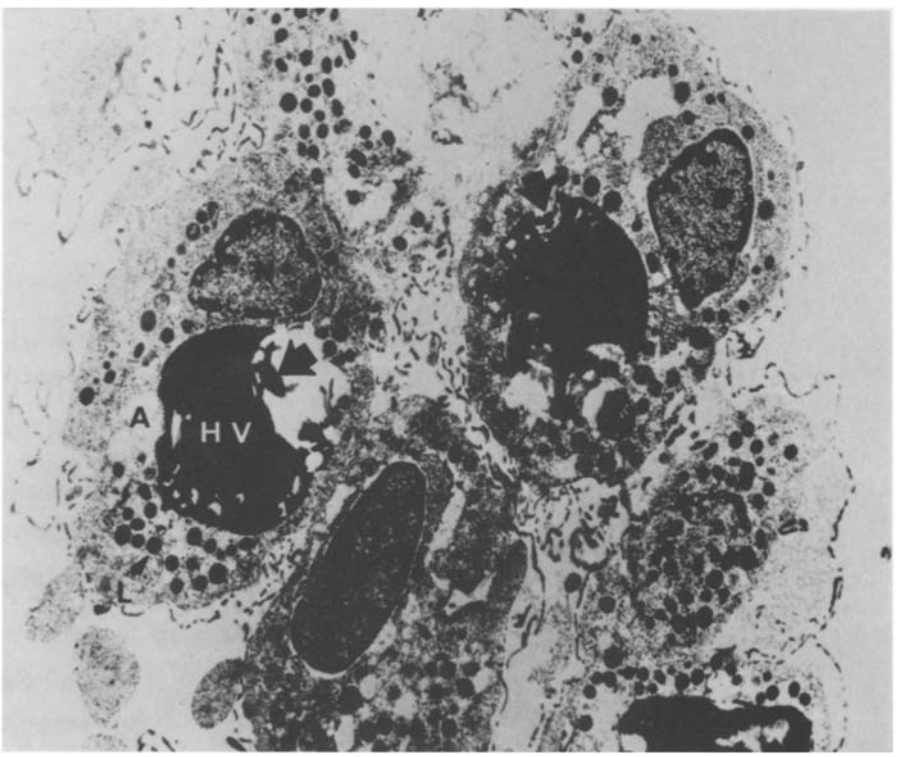

Figure 9. *L. puber*. Chromium-exposed amoebocytes. Electron micrograph showing several amoebocytes (A) with heterophagic vacuoles (HV) containing large electron dense chromium phosphate deposits (arrows), lysosomes (L) and nuclei (N); ×6440.

Figure 10. *L. puber*. Chromium-exposed digestive cells. Ion microscope spectrum. High mass resolution at 52^+ showing the small peak of chromium, corresponding to constitutive chromium and the large peak of CaC corresponding to a high contribution of polyatomic ions. I, intensity (A); M, mass.

performed at the cellular and subcellular levels: chromium was detected in gills, kidney, byssal threads, muscle and very faint concentrations in the digestive gland.

There are relatively a few studies which have clearly demonstrated the impact of chromium on crustacea and their ability to concentrate the metal. Data were obtained from the barnacle *Balanus amphitrite* (Barbaro *et al.* 1978), the crab *Podophthalmus vigil* (Sather 1967), the grass shrimp *Palaemonetes pugio* (Fales 1978, Doughtie *et al.* 1983, Doughtie & Rango Rao 1984); the two last papers demonstrate the structural and ultrastructural degenerative changes induced by hexavalant chromium in tissues such as the digestive gland, the gills and the mid gut. From our present study, no ultrastructural abnormalities were observed in nuclei and cellular organelles of gills, digestive gland and muscle. The trivalent chromium which was used as contaminant in *L. puber* was much less cytotoxic than the hexavalent salts which, moreover, have long been recognized as carcinogenic in other biological systems.

With regard to trace metal concentration in crustacea, it is generally agreed that the process of ecdysis, including the frequency of molting, is a prime confounder of trace metal metabolism interpretation, especially among decapods. This is the reason why investigations are required at the ultrastructural level. In the gills of chromium-exposed *L. puber*, the ion micrographs revealed the presence of chromium deposits at the cuticle level. These findings were then confirmed by observations made using electron microscopy associated with EMPA. The images indicated more precisely that chromium was only adsorbed onto the surface. No chromium could be detected in the inner part of the cuticle nor in the epithelial cell organelles such as lysosomes. According to our previous data, obtained from the gills of chromium-exposed mussels, epithelial cell lysosomes were shown to concentrate the metal.

Microanalytical data obtained from the shore crab *Carcinus maenas* demonstrated that other mineral contaminants such as uranium (Chassard-Bouchaud 1983) and thulium (Chassard-Bouchaud *et al.* 1984) were stored in gill epithelium lysosomes. In the present case, the gill cuticle of *L. puber* acts as a barrier preventing the penetration of chromium salts. Moreover, at molting, when the old exoskeleton is shed off, the crab can easily detoxicate.

Our data show chromium adsorption on the crab cuticle in agreement with other reports. Watson *et al.* (1970), who indicated that, on a given contaminated area, fish generally contained lower chromium concentrations than benthic invertebrates, suggested that the higher chromium levels in benthos living specimens were due to surface adsorption rather than assimilation of chromium into cells and tissues. Sequestering of metals at the body surface has been suggested as an adaptative mechanism preventing the accumulation of these materials internally to levels that may be toxic (Giesy & Wiener 1977, Bryan & Hummerstone 1973).

In the digestive gland of chromium-exposed *L. puber*, as well as in the gills, lysosomes were completely free of chromium. From our previous data, low chromium levels were detected in lysosomes of the mussel digestive gland, which is known to be the main organ of metal concentration in most invertebrates and, particularly, in crustacea and in bivalves which concentrate aluminium (Chassard-Bouchaud & Galle 1986), silver, lead (Chassard-Bouchaud *et al.* 1985) or uranium (Chassard-Bouchaud & Escaig 1984) in that tissue. In the digestive gland of cadmium-exposed crayfish *Pontastacus leptodactylus*, metal was stored in lysosomes (Chassard-Bouchaud 1981) and in the digestive gland of cadmium-exposed shore crab *C. maenas*, metal was stored in spherocrystals (Chassard-Bouchaud 1982). In the case of *L. puber*, no chromium was detected in any digestive gland organelle.

The muscle of *L. puber* was the only tissue with intracellular chromium appearing as dense precipitates. Similar results were obtained from *M. edulis*, where non-membrane limited chromium microprecipitates were detected lying within myofibrills. In crustacea such as the crayfish *Procambarus clarkii* (Hernandez *et al.* 1986) and in the crab *Xantho hydrophilus* (Peternac & Legovic 1986), chromium occurred in the mucle. Chromium has also been detected in the muscle tissue of several teleost fish (Plaskett & Potter 1979, Elwood *et al.* 1980). Our present data demonstrating chromium concentration in *L. puber* muscle are consistent with our data obtained from *M. edulis* muscle

and with results achieved by several other authors on crustacea, and fish muscles. The muscle is a chromium concentration site because chromium is bound to tissue proteins (Hoss & Baptist 1973, Descamps & Foulquier 1974). Human consumption of the muscle portion—the only edible part of *L. puber* collected from chromium contaminated water would present a possible health hazard.

Amoebocytes are well known to be special cells involved in the phagocytic clearance of pollutants (Read & Read 1972) as they can perform both intra and extracellular digestion of foreign particles. They migrate to the digestive gland and other epithelial linings such as gills where they are discharged to the exterior. They are enzymatically equipped with lysosomal phosphatase, a fact which is in agreement with the finding that chromium associated with phosphorus was detected from their heterophagic vacuoles in *L. puber*. Chromium phosphate was the result of an enzymatic reaction of acid phosphatase activity, as demonstrated by a method based on its microanalytical visualization (Berry *et al.* 1982). When sequestering chromium, lysosomes play a defensive role by preventing the diffusion of the toxic metal throughout the cell. Our present data refering to crab amoebocytes are in agreement with ours obtained from chromium-exposed mussels and with those published by George *et al.* (1978) on the oyster *Ostrea edulis* and by George & Pirie (1980) on *M. edulis*, who demonstrated the role of amoebocytes in performing detoxication of metals.

In conclusion, chromium trivalent salts do not seem to induce cellular alterations in the tissues of *L. puber*. The digestive gland is not the target organ of chromium bioaccumulation in that species, as its epithelial cells organelles, lysosomes and spherocrystals are free of chromium. The only instracellular concentration site of chromium was demonstrated to be myofibrills. Chromium precipitates were simply adsorbed onto the surface of the exoskeleton, assuming a passive detoxication at molting. Amoebocytes, which are the main target cells of chromium bioaccumulation, can assume an active detoxication.

From our data, it appears that *L. puber* cannot be considered as a suitable biological indicator of chromium pollution, because like all the arthropods, it has to molt. Few aspects of crustacean physiology are as important as molting. Basically a means of growth for an organism with an exoskeleton, it is in fact a process which dominates the crustacean's life. The whole metabolism is affected both directly and indirectly by these periodic replacements of the integument and their underlying cycles of metabolite and mineral accumulation (Chassard-Bouchaud 1972).

Acknowledgments

This work was financially supported by the Food and Agriculture Organization of the United Nations: MED POL II Programme (contract FRA 24 G), by the National Science Foundation of the United States (grant BBS-8610518) and by INSERM France (S.C27). We are indebted to Professor P. Galle for critical reading of the manuscript. Electron microscopy was performed in the Centre Interuniversitaire de Microscopie Electronique, CIME, 7 Quai Saint Bernard, 75252 Paris Cedex 05, France.

References

Allan IA. 1988 Etude par microanalyse chimique et par mesures isotopiques du devenir du chrome inhalé sous forme d'aérosols de différentes solubilités. *Thèse Doctorat*, Université Paris XII.

Barbaro A, Francescon A, Polo B, Bilio M. 1978 *Balanus amphitrite* (Cirripedia: Thoracica)–a potential indicator of fluorine, copper, lead, chromium and mercury in north Adriatic lagoons. *Mar Biol* **46,** 247–257.

Bernhard M, Zattera A. 1975 Major pollutants in the marine environment. In: Pearson A, Frangipane P, eds. *Marine Pollution and Marine Waste Disposal*. New York: Pergamon; 195–300.

Berry JP, Hourdry J, Sternberg M, Galle P. 1982 Aluminium phosphate visualisation of acid phosphatase activity: a biochemical and X-ray microanalysis study. *J Histochem Cytochem* **30,** 86–90.

Bryan GW, Hummerstone G. 1973 Adaptation of the polychaete *Nereis diversicolor* to estuarine sediments containing high concentration of zinc and cadmium. *J Mar Biol Ass UK* **53,** 839–857.

Castaing R, Slodzian G. 1962 Microanalyse par émission ionique secondaire. *J Microsc* **1,** 395–410.

Chassard-Bouchaud C. 1972 Analyse chimique des chromatophores de *Crangon crangon* (Linné) (Crustacé Décapode) par spectrographie des rayons X. Différences quantitatives de composition en éléments Ca, P, S et Mg au cours du cycle d'intermue. *C R Acad Sci Paris* **274,** 2511–2514.

Chassard-Bouchaud C. 1981 Rôle des lysosomes dans le phénomène de concentration du cadmium. Microanalyse par spectrographie des rayons X. *C R Acad Sci Paris* **293,** série III, 61–265.

Chassard-Bouchaud C. 1982 Localisation ultrastructurale du cadmium dans la glande digestive du crabe *Carcinus maenas* (Crustacé Décapode). Microanalyse par spectrographie des rayons X. *C R Acad Sci Paris* **294,** séie III, 153–157.

Chassard-Bouchaud C. 1983 Cellular and subcellular localization of uranium in the crab *Carcinus maenas*: a microanalytical study. *Mar Pollut Bull* **14,** 133 136.

Chassard-Bouchaud C. 1991 Microanalytical techniques in toxicological investigations. In Abel PD, Axiak V, eds. *Ecotoxicology and the Marine Environment*. New York: Ellis Horwood; 176–200.

Chassard-Bouchaud C. 1993 Criteria for the selection of organisms for monitoring purposes. *FAO/UNEP/IAEA Design of Monitoring Programmes and Management of Data concerning Chemical Contaminants in Marine Organisms*: 137–150.

Chassard-Bouchaud C, Escaig F. 1984 Uptake, storage and excretion of uranium by *Mytilus edulis*. A structural, ultrastructural and microanalytical study by secondary ion mass and X-ray spectrometry. *J Phys* **45,** C2, 545–548.

Chassard-Bouchaud C, Galle P. 1986 Bioaccumulation d'aluminium par les organisms marins. Mise en évidence par microscopie corpusculaire analytique. *C R Acad Sci Paris* **302,** série III, 55–61.

Chassard-Bouchaud C, Hallégot P, Meignan M. 1984 Thulium bioaccumulation by the shore crab *Carcinus maenas* collected from the French coasts of the Channel: a structural, ultrastructural and microanalytical study by secondary ion mass and X-ray spectrometry. *J Phys* **45,** C2, 541–544.

Chassard-Bouchaud C, Galle P, Escaig F. 1985 Mise en évidence d'une contamination par l'argent et le plomb de l'huitre

Crassostrea gigas et de la moule *Mytilus edulis* dans les eaux côtières françaises. Etude microanalytique par émission ionique secondaire. *C R Acad Sci Paris* **300,** série III, 3–8.

Chassard-Bouchaud C, Boutin JF, Hallegot P, Galle P. 1989 Chromium uptake, distribution and loss in the mussel *Mytilus edulis*: a structural, ultrastructural and microanalytical study. *Dis Aquat Org* **7,** 117–136.

Chassard-Bouchaud C, Escaig F, Galle P. 1992 Microanalysis and image processing of stable and radioactive elements in ecotoxicology. Current developments using SIMS microscope and electron microprobe. *Biol Cell* **74,** 59–74.

De Clerck R, Vanderstappen R, Vyncke W, Van Hoeyweghen P. 1979 Teneur en métaux lourds dans les organismes marins provenant de la capture accessoire de la pêche côtière belge. *Rev de L'Agric* **3,** 793–801.

Descamps B, Foulquier L. 1974 Aperçu sur la contamination expérimentale d'*Anguilla anguilla* (L.) par le chrome 51. *Rapport CEA-R-4548.* Centre d'Etudes Nucléaires de Cadarache, Département de Protection, Laboratoire de Radioécologie Continentale.

Doughtie DG, Conklin PJ, Rao KR. 1983 Cuticular lesions induced in grass shrimp exposed to hexavalent chromium. *J Invertebr Pathol* **42,** 249–258.

Doughtie DG, Rao KR. 1984 Histopathological and ultrastructural changes in the antennal gland, midgut, hepatopancreas and gill of grass shrimp following exposure to hexavalent chromium. *J Invertebr Pathol* **43,** 89–108.

Drach P, Tchernigovtzeff C. 1967 Sur la méthode de détermination des stades d'intermue et son application générale aux Crustacès. *Vie et Milieu* A **18,** 595 610.

Elwood JW, Beauchamp JJ, Allen CP. 1980 Chromium levels in fish from a lake chronically contaminated with chromates from cooling towers. *Int J Environ Stud* **14,** 289–298.

Fales RR. 1978 The influence of temperature and salinity on the toxicity of hexavalent chromium to the grass shrimp *Palaemonetes pugio* (Holthuis). *Bull Environ Contam Toxicol* **20,** 447–450.

Fukai R, Broquet D. 1965 Distribution of chromium in marine oganisms. *Bull Inst Ocean Monaco* **65** (1336), 3–19.

George SG, Pirie BJS. 1980 Metabolism of zinc in the mussel *Mytilus edulis* (L.): a combined ultrastructural and biochemical study. *J Mar Biol Ass UK* **60,** 575–590.

George SG, Pirie BJS, Cheyne AR, Coombs TL, Grant PT. 1978 Detoxication of metals by marine bivalves: an ultrastructural study of the compartmentation of copper and zinc in the oyster *Ostrea edulis*. *Mar Biol* **45,** 147–156.

Giesy JP, Wiener JG. 1977 Frequency distribution of trace metal concentration in five freshwater fishes. *Trans Am Fish Soc* **106,** 393–403.

Grieg RA, Wenzloff DR, Adams A, Nelson B, Shelpuk C. 1977 Trace metals in organisms from ocean disposal sites of the middle eastern United States. *Arch Environ Contam Toxicol* **6,** 395–409.

Hernandez F, Diaz J, Medina J, Del Ramo J, Pastor A. 1986 Determination of chromium in treated crayfish, *Procambarus clarkii*, by electrothermal AAS: study of chromium accumulation in different tissues. *Bull Environ Contam Toxicol* **36,** 851–857.

Hoss DE, Baptist JP. 1973 Accumulation of soluble and particulate radionuclides by estuarine fish. In: Nelson F, ed. *Proc 3rd Natl Symp on Radioecology 2*, Conf-710501, Springfield, VI; 776–782.

Kieffer F. 1979 Trace elements govern our health. *Sandoz Bull* 51–53.

Langård S. 1982 Absorption, transport and excretion of chromium in man and animals. In: Langård S, ed. *Biological and Environmental Aspects of Chromium.* Amsterdam: Elsevier Biomedical; 149 169.

Nriagu JO, Pacyna JM. 1988 Quantitative assessment of worldwide contamination of air, water and soils by trace metals. *Nature* **333,** 134–139.

Outrequin M, Bernard JL, Inglebert RL. 1988 Detection limit optimization in the new MIQ 256 microprobe. In: Benninghoven A, Huber AM, Werner HW, eds. *Secondary Ion Mass Spectrometry—SIMS VI.* New York: John Wiley; 165–168.

Peternac B, Legovic T. 1986 Uptake, distribution and loss of chromium in the crab *Xantho hydrophilus*. *Mar Biol* **91,** 467 471.

Plaskett D, Potter IC. 1979 Heavy metal concentrations in the muscle tissue of 12 species of Teleost from Cockburn Sound, Western Australia. *Aust J Mar Freshwater Res* **30,** 607–616.

Read P, Read E. 1972 Phagocytosis in invertebrates. II. The clearance of carbon particles by the clam *Tridacna maxima*. *Res J Reticuloendothelial Soc* **12,** 349 360.

Sather BT. 1967 Chromium absorption and metabolism by the crab *Podophthalmus vigil*. In: Nelson DJ, Evans FC, eds. *Proc Int Symp Radioecol Concent Process*, Michigan: Ann Arbor; 943–976.

Strik JJ, De Longh HH, Vanrijn JW, White TP. 1975 *Sublethal Effects of Toxic Chemicals on Aquatic Animals.* Amsterdam: Elsevier.

Tennant DA, Forster WD. 1969 Seasonal variation and distribution of 65 Zn, 54 Mn and 51 Cr in tissues of the crab *Cancer magister* Dana. *Health Phys* **18,** 649–659.

Van As D, Fourie HO, Vleggaar CM. 1975 Trace element concentrations in marine organisms from the Cape West Coast. *South Afr J Sci* **71,** 151–154.

Watson DG, Cushing CE, Coutant CC, Templeton WL. 1970 Cycling of radionuclides in Columbia River biota. In: Hemphill GH, ed. *Trace Substances in Environmental Health.* Columbia: University of Missouri; 144–156.